Journal of Molecular Structure 1001 (2011) 36–42

Contents lists available at ScienceDirect

Journal of Molecular Structure

journal homepage: www.elsevier.com/locate/molstruc

Ruthenium(II) complexes: Cellular uptake, cytotoxicity, DNA-binding, photocleavage and antioxidant activity studies

Zheng-Zheng Li [a], Zhen-Hua Liang [a], Hong-Liang Huang [b,*], Yun-Jun Liu [a,*]

[a] School of Pharmacy, Guangdong Pharmaceutical University, Guangzhou 510006, PR China
[b] School of Life Science and Biopharmaceutical, Guangdong Pharmaceutical University, Guangzhou 510006, PR China

ARTICLE INFO

Article history:
Received 5 April 2011
Received in revised form 10 June 2011
Accepted 13 June 2011
Available online 17 June 2011

Keywords:
Ruthenium complexes
DNA-binding
Cytotoxicity
Cellular uptake
Antioxidant activity

ABSTRACT

Two new ruthenium(II) complexes $[Ru(dmp)_2(DNPIP)]^{2+}$ **1** and $[Ru(dmp)_2(DAPIP)]^{2+}$ **2** were synthesized and characterized. The DNA-binding behaviors of these complexes were investigated by absorption spectra, viscosity measurements and photocleavage. The DNA-binding constants for complexes **1** and **2** have been determined to be 6.24 (±0.11) × 10^4 and 1.64 (±0.49) × 10^4 M^{-1}. The results suggest that complexes **1** and **2** intercalate between the DNA base pairs. Binding stoichiometries were studied through a luminescence-based Job plot. The major inflection points for complexes **1** and **2** at $\chi = 0.31$ and $\chi = 0.51$ were observed. The data were consistent with 2:1 and 1:1 bp [complex]/[DNA] binding mode. Complex **1** shows higher activity than complex **2** against the selected tumor cell lines. In addition, the cellular uptake and antioxidant activity on hydroxyl radical were also explored.

1. Introduction

Ruthenium complexes are emerging as promising candidates for novel cancer therapies [1]. Two Ru-based drugs are in clinical development: (ImH)[trans-$RuCl_4$(DMSO)(Im)] (Im = imidazole) (NAMI-A) is effective against lung metastases [2–6], and KP1019 [(IndH)[trans-$RuCl_4(Ind)_2$]) (Ind = indazole)] is active against colon carcinomas [7–13] and DNA has been proposed as a possible important target [12]. Thus, studies on the binding of Ru(II) complexes with DNA have attracted great interest. A great progress has been made in the research of ruthenium(II) complexes binding with DNA in the last two decades. The results show that ruthenium(II) complexes can bind DNA in a noncovalence such as electrostatic binding, groove binding and intercalative mode. On the other hand, many ruthenium (II) polypyridyl complexes exert rather potent activities against selected tumor cells [14–16]. In our previous work [17], we found complexes containing 2,2′-bipyridine as ancillary have low cytotoxicity against the selected cell lines. To observe the cytotoxic effect of ruthenium(II) complexes containing different ancillary on the same tumor cell lines, in this article, we report the synthesis, characterization, DNA-binding, cytotoxicity, cellular uptake in vitro and antioxidant activity of two new ruthenium(II) complexes $[Ru(dmp)_2(DNPIP)](ClO_4)_2$ **1** (DNPIP = 2-(2,4-dinitrophenyl)imidazo[4,5-*f*][1,10]phenanthroline, dmp = 2,9-dimethyl-1,10-phenanthroline) and $[Ru(dmp)_2(DAPIP)](ClO_4)_2$ **2** (DAPIP = 2-(2,4-diaminophenyl)imidazo[4,5-*f*][1,10] phenanthroline, Scheme 1). The DNA-binding behaviors of these complexes were investigated by viscosity measurements, electronic absorption titration, and photoactivated cleavage. The cytotoxicity of these complexes was evaluated by MTT (3-(4,5-dimethylthiazol-2-yl)-2,5-diphenyltetrazolium bromide) assay. The cellular uptake was investigated and the experiments on antioxidant activity of these complexes against hydroxyl radical (·OH) was also explored.

2. Experimental

2.1. Materials and methods

Calf thymus DNA (CT-DNA) was obtained from the Sino-American Biotechnology Company. pBR322 DNA was obtained from Shanghai Sangon Biological Engineering & Services Co., Ltd. Dimethyl sulfoxide (DMSO) and RPMI 1640 were purchased from Sigma. Cell lines of hepatocellular (BEL-7402), hepatocellular (Hepg-2) and breast cancer (MCF-7) were purchased from American Type Culture Collection, agarose and ethidium bromide were obtained from Aldrich. $RuCl_3 \cdot xH_2O$ was purchased from Kunming Institution of Precious Metals. 1,10-Phenanthroline was obtained from Guangzhou Chemical Reagent Factory. Doubly distilled water was used to prepare buffers (5 mM Tris(hydroxymethylaminomethane)–HCl, 50 mM NaCl, pH = 7.2). A solution of calf thymus DNA in the buffer gave a ratio of UV absorbance

* Corresponding authors.
E-mail addresses: honglianghuangcn@hotmail.com (H.-L. Huang), lyjche@163.com (Y.-J. Liu).

0022-2860/$ - see front matter Crown Copyright © 2011 Published by Elsevier B.V. All rights reserved.
doi:10.1016/j.molstruc.2011.06.011

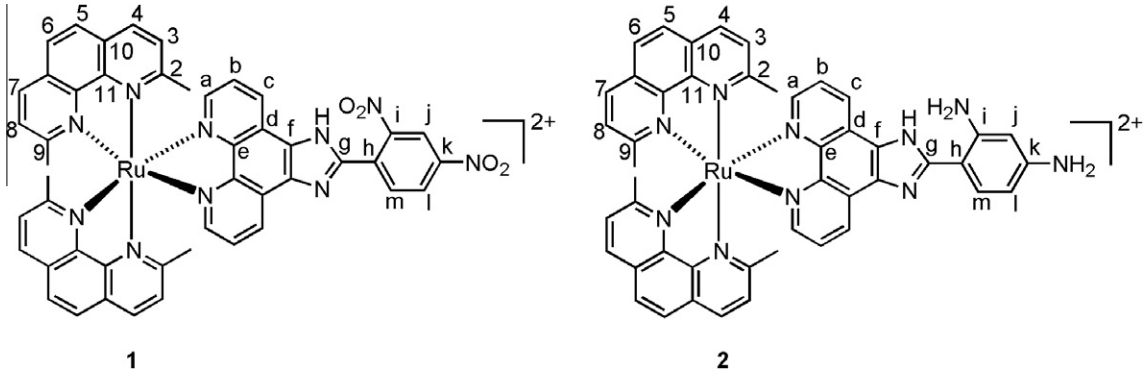

Scheme 1. The structure of complexes.

at 260 and 280 nm of ca. 1.8–1.9:1, indicating that the DNA was sufficiently free of protein [18]. The DNA concentration per nucleotide was determined by absorption spectroscopy using the molar absorption coefficient (6600 M^{-1} cm^{-1}) at 260 nm [19].

Microanalysis (C, H, and N) was carried out with a Perkin-Elmer 240Q elemental analyzer. Fast atom bombardment (FAB) mass spectra were recorded on a VG ZAB-HS spectrometer in a 3-nitrobenzyl alcohol matrix. Electrospray mass spectra (ES-MS) were recorded on a LCQ system (Finnigan MAT, USA) using methanol as mobile phase. The spray voltage, tube lens offset, capillary voltage and capillary temperature were set at 4.50 kV, 30.00 V, 23.00 V and 200 °C, respectively, and the quoted *m/z* values are for the major peaks in the isotope distribution. ^{1}H NMR and ^{13}C NMR spectra were recorded on a Varian-500 spectrometer. All chemical shifts were given relative to tetramethylsilane (TMS). UV/Vis spectra were recorded on a Shimadzu UV-3101PC spectrophotometer and emission spectra were recorded on a Shimadzu RF-4500 luminescence spectrometer at room temperature.

2.2. Synthesis and characterization

2.2.1. Synthesis of ligand (DNPIP)

The ligand DNPIP was synthesized according to literature [17]. A mixture of 1,10-phenanthroline-5,6-dione (0.315 g, 1.5 mmol) [20], 2,4-dinitrobenzaldehyde (0.294 g, 1.5 mmol), ammonium acetate (2.31 g, 30 mmol) and glacial acetic acid (20 cm^3) was refluxed with stirring for 2 h. The cooled solution was diluted with water and neutralized with concentrated aqueous ammonia. The precipitate was collected and purified by column chromatography on silica gel (60–100 mesh) with ethanol as eluent to give the compound as yellow powder. Yield: 80%. Anal. Calcd. for $C_{19}H_{10}N_6O_4$: C, 59.07; H, 2.61; N, 21.75; Found: C, 59.01; H, 2.54; N, 21.53%. FAB-MS: m/z = 387 $[M + H]^+$. ^{1}H NMR (500 MHz, DMSO–d_6): 9.08 (d, 1H, *J* = 8.2 Hz), 8.91 (d, 2H, *J* = 8.0 Hz), 8.79 (d, 1H, *J* = 8.5 Hz), 8.75 (d, 1H, *J* = 8.0 Hz), 8.44 (d, 2H, *J* = 8.5 Hz), 7.87 (dd, 2H, *J* = 5.5 Hz, *J* = 5.0 Hz). ^{13}C NMR (DMSO-d_6, ppm): 148.24 C (a), 147.09 C (k), 144.59 C (i), 143.90 C (e), 132.11 C (g), 131.22 C (h), 130.11 C (c), 128.93 C (l), 127.14 C (d), 126.09 C (m), 124.16 C (f), 123.41 C (b), 119.84 C (j).

2.2.2. Synthesis of [Ru(dmp)$_2$(DNPIP)](ClO$_4$)$_2$ (1)

A mixture of *cis*-[Ru(dmp)$_2$Cl$_2$]·2H$_2$O (0.312 g, 0.5 mmol) [21] and DNPIP (0.193 g, 0.5 mmol) in ethylene glycol (20 cm^3) was refluxed under argon for 8 h to give a clear red solution. Upon cooling, a red precipitate was obtained by dropwise addition of saturated aqueous $NaClO_4$ solution. The crude product was purified by column chromatography on a neutral alumina with a mixture of CH_3CN–toluene (3:1, v/v) as eluent. The main red band was collected. The solvent was removed under reduced pressure and a red powder was obtained. Yield: 71%. Anal. Calcd. for $C_{47}H_{34}N_{10}Cl_2O_{12}Ru$: C, 51.19; H, 3.11; N, 12.70; Found: C, 51.43; H, 3.02; N, 13.11%. ES-MS [CH_3CN, m/z]: 902.5 ($[M–2ClO_4–H]^+$), 451.6 ($[M–2ClO_4]^{2+}$). ^{1}H NMR (500 MHz, DMSO-d_6): δ 8.90 (d, 1H, *J* = 8.5 Hz), 8.60 (d, 2H, *J* = 8.5 Hz), 8.44 (dd, 4H, *J* = 6.5 Hz, *J* = 4.5 Hz), 8.23 (d, 2H, *J* = 8.5 Hz), 7.97 (d, 1H, *J* = 8.2 Hz), 7.37 (d, 1H, *J* = 8.5 Hz), 7.31 (dd, 4H, *J* = 7.5 Hz, *J* = 5.5 Hz), 7.24 (t, 2H, *J* = 5.5 Hz), 7.14–7.18 (m, 4H), 2.50 (s, 6H), 2.30 (s, 6H). ^{13}C NMR (DMSO-d_6, ppm): 167.71 C (2,9), 166.09 C (a), 148.97 C (k), 148.23 C (i), 147.94 C (e), 144.96 C (g), 137.81 C (11), 136.47 C (h), 130.48 C (c), 129.97 C (4,7), 129.39 C (l), 128.84 C (d), 128.14 C (m), 127.16 C (f), 126.40 C (10), 125.76 C (5,6), 125.45 C (3,8), 124.18 C (b), 118.93 C (j), 24.44 C (Me).

2.2.3. Synthesis of [Ru(dmp)$_2$(DAPIP)](ClO$_4$)$_2$ (2)

[Ru(dmp)$_2$(DNPIP)](ClO$_4$)$_2$ (0.552 g, 0.5 mmol) was completely dissolved in minimum amount of acetonitrile, then the Pd/C (0.20 g, 10% Pd), $NH_2NH_2·H_2O$ (8 cm^3) and ethanol (20 cm^3) were added in the above solution and refluxed under argon for 8 h. The hot solution was filtered and evaporated under reduced pressure to remove the solvent to 6 cm^3. Upon cooling, a red precipitate was obtained by dropwise addition of saturated aqueous $NaClO_4$ solution. The crude product was purified by column chromatography on a neutral alumina with a mixture of CH_3CN–toluene (3:1, v/v) as eluent. The red band was collected. The solvent was removed under reduced pressure and a red powder was obtained. Yield: 70%. Anal. Calcd. for $C_{47}H_{38}N_{10}Cl_2O_8Ru$: C, 54.13; H, 3.67; N, 13.43; Found: C, 53.94; H, 3.45; N, 13.82%. ES-MS [CH_3CN, m/z]: 842.3 ($[M–2ClO_4–H]^+$), 421.8 ($[M–2ClO_4]^{2+}$). ^{1}H NMR (500 MHz, DMSO-d_6): δ 8.91 (d, 2H, *J* = 8.5 Hz), 8.77 (dd, 4H, *J* = 8.5 Hz, *J* = 8.5 Hz), 8.24 (d, 2H, *J* = 8.5 Hz), 7.98 (d, 4H, *J* = 8.5 Hz), 7.62 (d, 2H, *J* = 8.0 Hz), 7.48 (t, 1H, *J* = 6.0 Hz), 7.38 (d, 4H, *J* = 8.5 Hz), 7.31 (d, 1H, *J* = 4.0 Hz), 6.01 (d, 1H, *J* = 5.5 Hz), 5.42 (s, 4H), 1.94 (s, 6H), 1.70 (s, 6H). ^{13}C NMR (DMSO-d_6, ppm): 167.87 C (2,9), 166.30 C (a), 155.13 C (e), 151.46 C (k), 149.61 C (i), 148.85 C (g), 147.77 C (11), 145.14 C (c, 4,7), 138.00 C (m,d), 136.59 C (f,10), 129.45 C (5,6), 127.31 C (3,8), 126.45 C (b), 124.89 C (h), 103.93 C (l), 98.64 C (j), 24.45 C (Me).

Caution: Perchlorate salts of metal compounds with organic ligands are potentially explosive, and only small amounts of the material should be prepared and handled with great care.

2.3. DNA binding and photoactivated cleavage

The DNA-binding and photoactivated cleavage experiments were performed at room temperature. Buffer A [5 mM Tris(hydroxymethyl)aminomethane (Tris) hydrochloride, 50 mM NaCl, pH 7.0] was used for absorption titration, luminescence titration and viscosity measurements. Buffer B (50 mM Tris–HCl,

18 mM NaCl, pH 7.2) was used for DNA photocleavage experiments.

The absorption titrations of the complex in buffer were performed using a fixed concentration (20 μM) for complex to which increments of the DNA stock solution were added. Ru-DNA solutions were incubated for 5 min before the absorption spectra were recorded. The intrinsic binding constants K, based on the absorption titration, were measured by monitoring the changes of absorption in the metal-to-ligand transfer (MLCT) band with increasing concentration of DNA using the following equation [22].

$$\frac{[DNA]}{\varepsilon_a - \varepsilon_f} = \frac{[DNA]}{\varepsilon_b - \varepsilon_f} + \frac{1}{K_b(\varepsilon_b - \varepsilon_f)} \quad (1)$$

where [DNA] is the concentration of DNA in base pairs, ε_a, ε_f and ε_b correspond to the apparent absorption coefficient Aobsd/[Ru], the extinction coefficient for the free ruthenium complex and the extinction coefficient for the ruthenium complex in the fully bound form, respectively. In plots of [DNA]/(ε_a–ε_f) versus [DNA], K_b is given by the ratio of slope to the intercept.

Viscosity measurements were carried out using an Ubbelodhe viscometer maintained at a constant temperature at 25.0 (±0.1) °C in a thermostatic bath. DNA samples about 200 bp in average length were prepared by sonication to minimize complexities arising from DNA flexibility [23]. Flow time was measured with a digital stopwatch, and each sample was measured three times, and an average flow time was calculated. Relative viscosities for DNA in the presence and absence of complexes were calculated from the relation $\eta = (t - t^0)/t^0$, where t is the observed flow time of the DNA-containing solution and t^0 is the flow time of buffer alone [24,25]. Data are presented as $(\eta/\eta_0)^{1/3}$ versus binding ratio [26], where η is the viscosity of DNA in the presence of complexes and η_0 is the viscosity of DNA alone.

For the gel electrophoresis experiment, supercoiled pBR322 DNA (0.1 μg) was treated with the Ru(II) complexes in buffer B, and the solution was then irradiated at room temperature with a UV lamp (365 nm, 10 W). The samples were analyzed by electrophoresis for 1.5 h at 80 V on a 0.8% agarose gel in TBE (89 mM Tris–borate acid, 2 mM EDTA, pH = 8.3). The gel was stained with 1 μg/ml ethidium bromide and photographed on an Alpha Innotech IS–5500 fluorescence chemiluminescence and visible imaging system.

2.4. Continuous variation analysis

Binding stoichiometries were obtained for complexes **1** and **2** with CT DNA using the method of continuous variation [27]. The concentrations of both complex and DNA were varied, while the sum of the reactant concentrations was kept constant at 50 μM (in terms of base pairs for the DNA). Solutions of complexes and DNA were prepared in Tris–HCl buffer (pH = 7.4). In the sample solutions, the mole fraction χ of complex was varied from 0 to 1.0 in 0.1 ratio steps. The fluorescence intensities of these mixtures were measured at 25 °C using an excitation wavelength of 460 nm. The intensity in fluorescence was plotted versus the mole fraction χ of complex to generate a Job plot. Linear regression analysis of the data was performed in the software of Origin 7.0.

2.5. Detecting the formation of singlet oxygen photo-induced by complexes

A 3 ml N,N-dimethylformamide (DMF) solution containing complexes (10 μM) and 9,10-dimethylanthracene (DMA, 100 μM) was prepared in a quartz cuvette, and the initial absorbance (A_0) at 399 nm of this solution was recorded on a Shimadzu UV-3101PC spectrophotometer with 10 μM complexes **1** and **2** as reference solution, then the cuvette was irradiated for 30 min with the monochromatic UV lamp (λ = 365 nm), its absorbance (A) at 399 nm was taken immediately. In the same way, the A_0 and A of 10 μM complex **1** and **2**, as well as the A_0 and A of 100 μM DMA were measured with the solvent DMF as a blank. All the records were made three times and expressed as the average value.

2.6. Cell culture and cytotoxicity assay in vitro

Standard 3-(4,5-dimethylthiazole)-2,5-diphenyltetraazolium bromide (MTT) assay procedures were used [28]. Cells were placed in 96-well microassay culture plates (8×10^3 cells per well) and grown overnight at 37 °C in a 5% CO_2 incubator. The complexes tested were dissolved in DMSO and diluted with RPMI 1640 and then added to the wells to achieve final concentrations ranging from 10^{-6} to 10^{-4} M. Control wells were prepared by addition of culture medium (100 μL). Wells containing culture medium without cells were used as blanks. The plates were incubated at 37 °C in a 5% CO_2 incubator for 72 h. Upon completion of the incubation, stock MTT dye solution (20 μL, 5 mg mL^{-1}) was added to each well. After 4 h, buffer (100 μL) containing N,N-dimethylformamide (50%) and sodium dodecyl sulfate (20%) was added to solubilize the MTT formazan. The optical density of each well was then measured on a microplate spectrophotometer at a wavelength of 490 nm. The IC_{50} values were determined by plotting the percentage viability versus concentration on a logarithmic graph and reading off the concentration at which 50% of cells remain viable relative to the control. Each experiment was repeated at least three times to get the mean values. Three different tumor cell lines were the subjects of this study: BEL-7402, Hepg-2 and MCF-7 (purchased from American Type Culture Collection).

2.7. Celluar uptake study

Cells were placed in 24-well microassay culture plates (4×10^4 cells per well) and grown overnight at 37 °C in a 5% CO_2 incubator. Compounds tested (50 μM) were then added to the wells. The plates were incubated at 37 °C in a 5% CO_2 incubator for 48 h. Then, the wells were washed three times with phosphate buffered saline (PBS), and after removing the culture media, the cells were visualized by fluorescent microscopy.

2.8. Antioxidant activity

The hydroxyl radical (·OH) in aqueous media was generated by the Fenton system [29]. The solution of the tested complexes was prepared with DMF (N,N-dimethylformamide). The assay mixture (5 mL) contained following reagents: safranin (28.5 μM), EDTA-Fe(II) (100 μM), H_2O_2 (44.0 μM), the tested compounds (0.5–4.5 μM) and a phosphate buffer (67 mM, pH = 7.4). The assay mixtures were incubated at 37 °C for 30 min in a water bath. Then the absorbance was measured at 520 nm. All the tests were run in triplicate and expressed as the mean. A_i was the absorbance in the presence of the tested compound; A_0 was the absorbance in the absence of tested compounds; A_c was the absorbance in the absence of tested compound, EDTA-Fe(II), H_2O_2. The suppression ratio (η_a) was calculated on the basis of (A_i–A_0)/(A_c–A_0) × 100%.

3. Results and discussion

3.1. Electronic absorption titration

The electronic absorption spectra of complexes **1** and **2** mainly consist of two or three resolved bands. The band below 300 nm is attributed to intraligand (IL) $\pi \rightarrow \pi*$ transition, the band at 345–

350 nm is attributed to $\pi \rightarrow \pi*$ transition, and the low energy absorption band centered at 455–465 nm is assigned to metal-to-ligand charge transfer (MLCT) transition by comparison with the spectrum of other polypyridyl Ru(II) complexes [30–32]. Addition of CT DNA to buffered aqueous solution of the complexes produces distinctive changes in their absorption spectra. The absorption spectra of complexes **1** and **2** in the absence and presence of CT DNA are given in Fig. 1. As the DNA concentration is increased, the MLCT transition bands of complexes **1** at 468 and **2** at 467 nm exhibit hypochromism of about 38.41 and 31.85%, and bathochromism of 2 nm, respectively. The intrinsic constants K_b for complexes **1** and **2** were determined by monitoring the changes in absorbance at the MLCT band with increasing concentration of CT DNA. The values of K_b are 6.24 $(\pm 0.11) \times 10^4$ and 1.64 $(\pm 0.49) \times 10^4\ M^{-1}$ for complexes **1** and **2**, respectively. The DNA-binding constant of complex **1** is larger than that of complex **2**, which is caused by the electron-withdrawing substituent ($-NO_2$ in DNPIP) on the intercalative ligand improving the DNA-binding affinity, and the electron-pushing substituent ($-NH_2$ in DAPIP) decreasing the DNA affinity. Similar results were observed for other ruthenium(II) complexes [33]. These values are comparable to that of complexes $[Ru(dmp)_2(maip)]^{2+}$ $(3.23 \times 10^4\ M^{-1})$ and $[Ru(dmp)_2(paip)]^{2+}$ $(4.34 \times 10^4\ M^{-1})$ [34], but is not as strong as that of $[Ru(bpy)_2(dppz)]^{2+}$ $(4.9 \times 10^6\ M^{-1}$, dppz = dipyrido[2,3-*a*:3′,2′-*c*]phenazine) [35].

3.2. Viscosity measurements

It is well-established that intercalation results in a lengthening of DNA, thus producing increases in relative specific viscosity of solution of DNA [23,36]. Therefore, to probe the nature of the interaction between the ruthenium complexes and DNA, the effect of the addition of the complexes **1** and **2** on the viscosity of aqueous CT DNA solutions was studied. Fig. 2 shows the changes in the relative viscosity of CT DNA on addition of complexes **1** and **2**. Upon increasing the amounts of complexes **1** and **2**, the relative viscosity of CT DNA solution increase steadily, which confirms that all these complexes interact with CT DNA through intercalative mode. The increased degree of viscosity depends on complex-DNA affinities, which followed the order of complex **1** > **2**.

3.3. Luminescence studies

Emission intensity of complexes **1** and **2** from their MLCT excited states upon exicitation at 468 and 467 nm is found to depend on DNA concentration. For each titration of CT DNA, luminescence enhancements occur within minutes of DNA addition, indicating that association rates are relatively rapid. As shown in Fig. 3, as

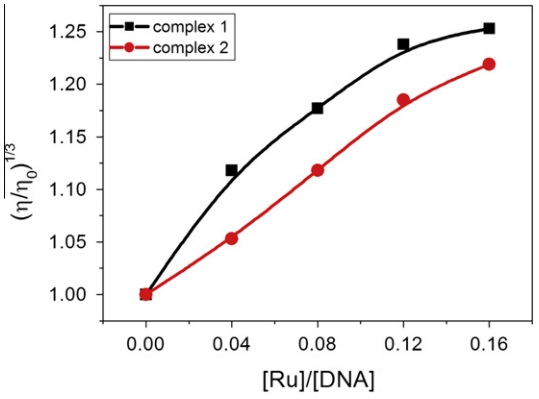

Fig. 2. Effect of increasing amounts of complexes **1** (■) and **2** (●) on the relative viscosity of calf thymus DNA at 25 (±0.1) °C. [DNA] = 0.25 mM.

the concentration of CT DNA increased, the emission intensities of complexes **1** (at 597 nm) and **2** (at 596 nm) were about 6.98 and 4.99 times larger than the original, respectively. This clearly indicates that complex **1** is in a more hydrophobic environment in the presence of DNA when compared to complex **2**.

3.4. Continuous variation analysis

Binding of complexes **1** and **2** to CT DNA was examined at 25 °C in Tris–HCl buffer by the method of continuous variation analysis to determine the overall stoichiometries. Fig. 4 shows normalized Job plots for DNA. The point of the intersection of two best fit lines in the Job plots for the complexes **1** and **2** with DNA are 0.31 and 0.51 that correspond to complex/DNA stoichiometries of 1:2 and 1:1, respectively.

3.5. Photoactivated cleavage of pBR322 DNA

It is well known when circular plasmid DNA is subjected to electrophoresis, relatively fast migration will be observed for the intact supercoiled form (Form I); If scission occurs on one strand (nicked), the supercoiled will relax to generate a slower-moving open circular form (Form II) [37]. As shown in Fig. 5a, No obvious DNA cleavage was observed for the control in which metal complex was absent (DNA alone), or incubation of the plasmid with the Ru(II) complexes in darkness. With increasing concentration of complexes, the Form I decrease and Form II increase gradually. Under the same experimental condition, complex **1** exhibits more effective DNA cleavage activity than complex **2**. The different

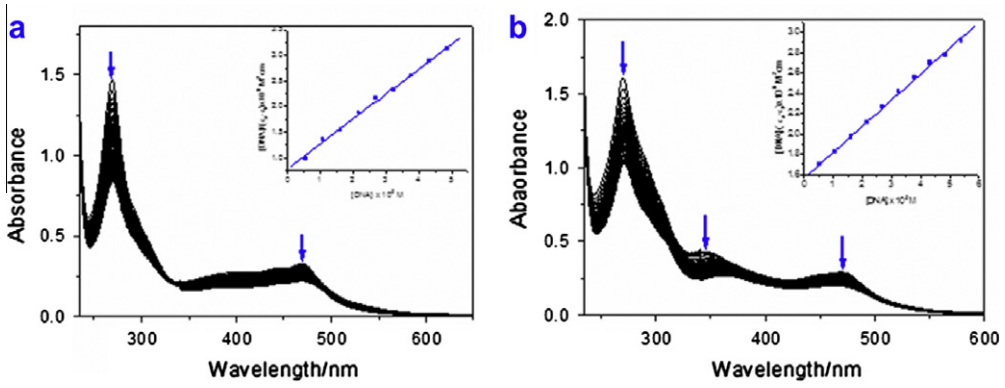

Fig. 1. Absorption spectra of complex **1** (a) and **2** (b) in Tris–HCl buffer upon addition of CT-DNA. [Ru] = 20 μM. Arrow shows the absorbance change upon the increase of DNA concentration. Plots of [DNA]/(ε_a–ε_f) versus [DNA] for the titration of DNA with Ru(II) complexes.

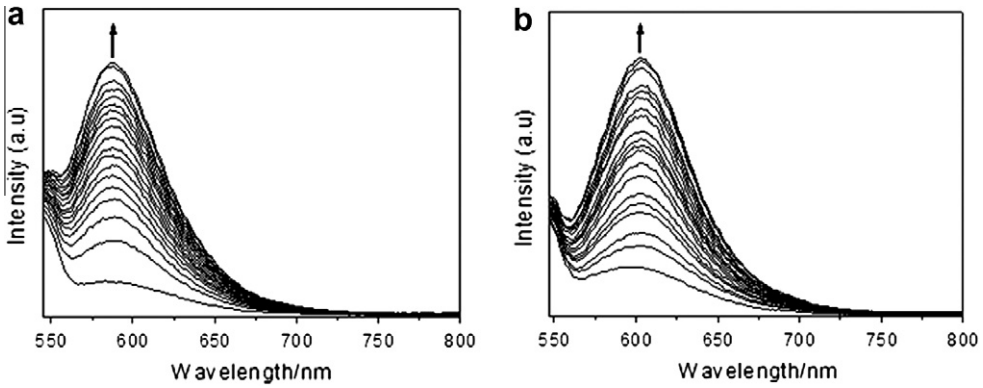

Fig. 3. Luminescence spectra of complexes **1** (a) and **2** (b) in Tris–HCl buffer upon addition of CT DNA. [Ru] = 5 μM. Arrow shows the intensity change upon the increase of DNA concentrations.

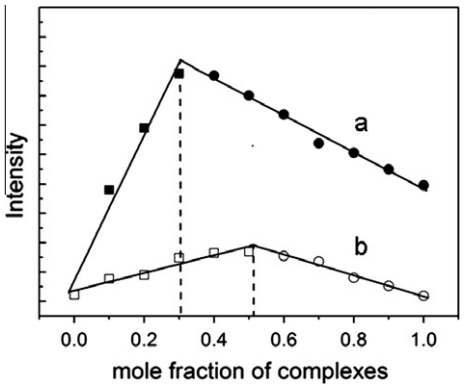

Fig. 4. Job plot using luminescence data for complexes 1 (a) and 2 (b) with CT DNA in Tris–HCl buffer, pH = 7.0.

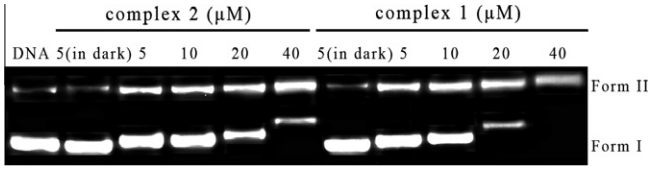

Fig. 5a. Photoactivated cleavage of pBR 322 DNA in the presence of different concentrations of Ru(II) complexes after irradiation at 365 nm for 30 min.

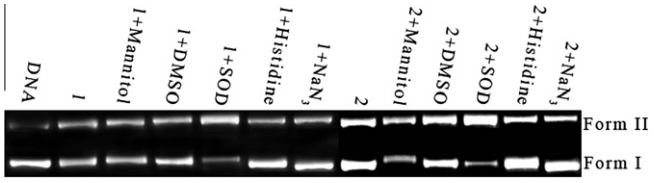

Fig. 5b. Photoactivated cleavage of supercoiled pBR 322 DNA by complexes **1** and **2** (20 μM) in the absence and presence of different inhibitors [100 mM mannitol, 200 mM dimethyl sulfoxide (DMSO), 1000 U ml^{-1} superoxide dismutase (SOD), 1.2 mM distidine] after irradiation at 365 nm for 30 min.

cleaving efficiency may be ascribed to the different binding affinity of two Ru(II) complexes to DNA.

In order establish the reactive species responsible for the photoactivated cleavage of the plasmid, the influence of different potentially inhibiting agents was investigated. Fig. 5b shows that the DNA cleavage of the plasmid by complexes **1** and **2** was not inhibited in the presence of hydroxyl radical (·OH) scavengers such as mannitol [29] and dimethylsulfoxide (DMSO) [38], which indicated that hydroxyl radical was not likely to be the cleaving agent. In the presence of superoxide dismutase (SOD), a facile superoxide anion radical ($O_2^{\cdot-}$) quencher, the cleavage was obviously improved. The DNA cleavage of the plasmid was inhibited in the presence of the singlet oxygen ($^1O_2$) scavenger histidine and NaN_3 [39,40], suggesting that $^1O_2$ is likely to be the reactive species responsible for the cleavage reaction.

Table 1
Absorbance at 399 nm for detecting the formation of singlet oxygen in the presence of complexes **1** and **2**.

		A_0	A	ΔA	$\Delta A_{DMA}-\Delta A_{complex}$
Complex	DMA	1.156	0.451	0.705	
	1	0.216	0.198	0.018	
	DMA + **1**	1.080	0.470	0.610	0.095
	2	0.206	0.185	0.021	
	DMA + **2**	1.041	0.485	0.556	0.149

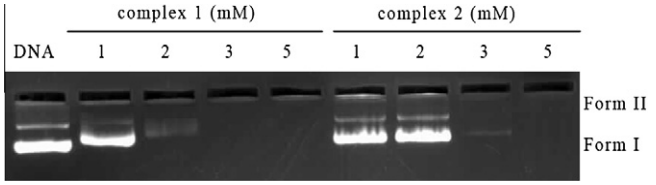

Fig. 6. Agarose gel electrophoresis retardation of pGL3 plasmid DNA by complexes **1** and **2**. [DNA] = 0.5 μg.

Table 2
The IC_{50} values for complexes **1** and **2** against selected cell lines.

Complex	IC50(μM)		
	BEL-7402	HepG-2	MCF-7
1	36.38 ± 3.28	32.79 ± 3.79	46.48 ± 3.24
2	77.07 ± 3.61	50.63 ± 3.91	96.41 ± 3.19
Cisplatin	19.78 ± 2.55	25.48 ± 3.15	12.24 ± 2.55

3.6. Detecting the generation of singlet oxygen

To detect the production of $^1O_2$ under irradiation at 365 nm in the presence of complexes **1** or **2**, the experiments were performed using 9,10-dimethylanthracene (DMA) as a quencher of single oxygen [41]. It is well known that DMA has a strong absorption at

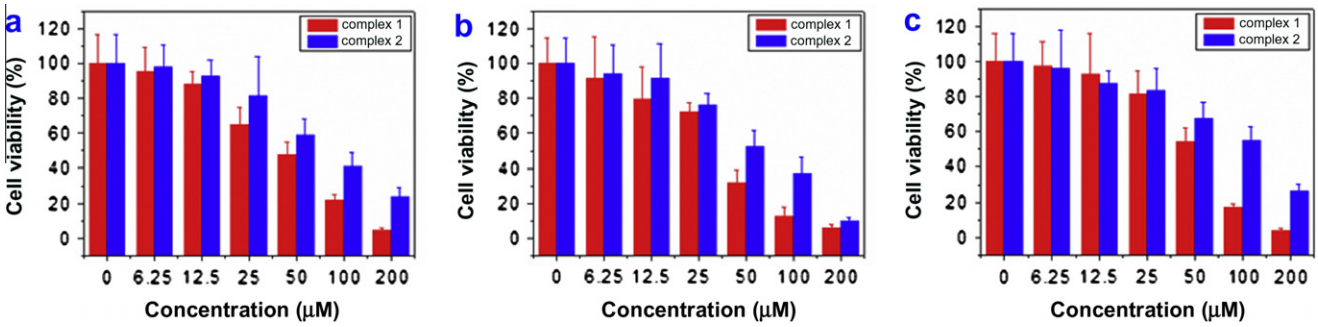

Fig. 7. Cell viability of complexes **1** and **2** on cell lines: BEL-7402 (a), Hepg-2 (b) and MCF-7 (c) in vitro. Each data point is the mean ± standard error obtained from at least three independent experiments.

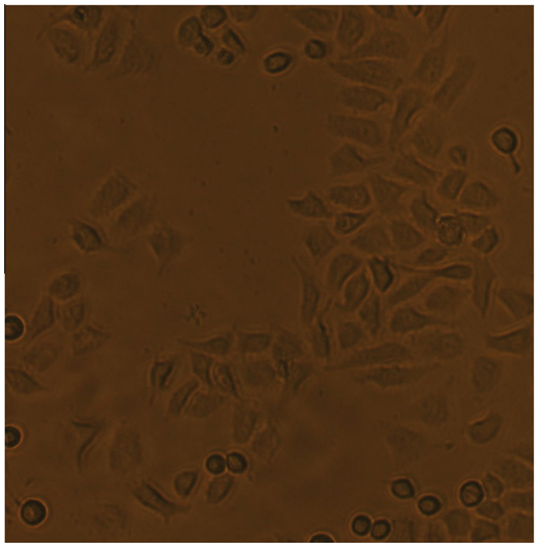

Fig. 8. BEL-7402 cells incubated with complexes **2** (50 μM) for 48 h. A imaged under fluorescence and visible light.

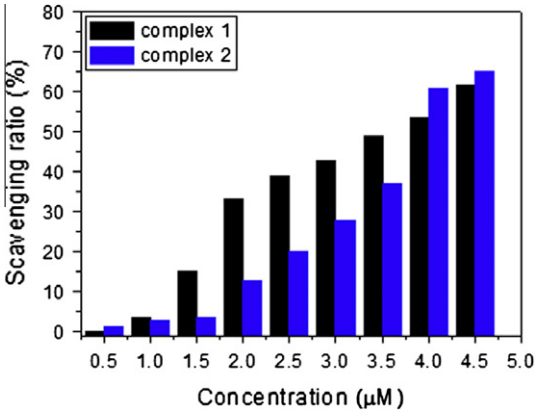

Fig. 9. Scanvenging effect of complexes **1** and **2** on hydroxyl radicals. Experiments were performed in triplicate.

399 nm, and this absorption will be photobleached upon chemical quenching reaction of DMA with $^1O_2$. The data were listed in Table 1. For complexes **1** and **2** alone, the absorbance changed little before and after irradiation, whereas for the mixture containing both DMA and complexes **1** or **2**, the change of ΔA was very obvious. The decrease in absorbance at 399 nm reflect the decrease in concentration of DMA. These results suggest that the generation of single oxygen is indeed occurred in the presence complexes **1** or **2** upon irradiation.

3.7. Retardation of pGL 3 DNA by Ru(II) complexes

Several studies reported the polyamine can condense DNA [42–44]. However, the studies of small molecules to condense DNA have been paid less attention. The large DNA-binding affinities of complexes **1** and **2** prompt us to consider if these complexes can effectively condense DNA into compact structures. Based on this hypothesis, the retardation of pGL 3 DNA by the two complexes was carried out. The effect on retardation was analyzed by agarose gel electrophoresis as shown in Fig. 6. when the concentrations of complexes **1** and **2** are 1 and 2 mM, complexes **1** and **2** can not condense the DNA, however, the concentrations reach 3 and 5 mM, the effects on condensation of DNA were observed.

3.8. Cytotoxicity assay in vitro

The IC_{50} values of the Ru(II) complexes **1** and **2** in three cell lines (BEL-7402, Hepg-2 and MCF-7) are listed in Table 2 and the cell viability is depicted in Fig. 7. The IC_{50} values for **1** and **2** range from 36.38 to 96.41 μM. Comparing the IC50 values of complex **1** and **2**, Complex **1** appeared to have higher cytotoxicity against all the selected cells than complex **2**, but cytotoxicity of the two Ru(II) complexes was relatively low when compared with cisplatin. Fig. 7 showed that the cell viability decreased with increasing concentration of complexes **1** and **2**. The results obtained showed that the cytotoxicity for complexes **1** and **2** against the selected tumor cell lines is consistent with the DNA-binding affinity.

3.9. Cellular uptake

Complex **2** (50 μM) was added to the well (4×10^4 cells per well). The plates were incubated at 37 °C in a 5% CO_2 incubator for 48 h. Then the well was washed three times with PBS, and the cells were observed under fluorescent microscopy. In the control experiment, BEL-7402 cells was not stained (data no presented). However, in the presence of complex **2**, the spots stained by complex **2** were observed in the image (Fig. 8). The results show complex **2** was successfully uptaken by BEL-7402 cells.

3.10. Antioxidant activity

In the last decade, a great deal of research has been devoted to the study of different types of antioxidants (natural and synthetic) which may at least minimize the deleterious effects induced by reactive oxygen species (ROS) [45]. It is well known that hydroxyl radical (·OH) can result in cell membrane disintegration and membrane protein damage. As shown in Fig. 9 and Table 3. the

Table 3
The scavenging ratios (%) of complexes against ·OH.

Comp	Average inhibition (%) for ·OH								
	0.5	1.0	1.5	2.0	2.5	3.0	3.5	4.0	4.5 (μM)
1	0.26	3.60	15.17	33.16	39.07	42.85	48.84	53.47	61.69
2	1.32	2.91	3.69	12.66	20.32	27.97	35.94	60.94	65.17

suppression ratio against ·OH ranged from 0.26% to 61.69% for complex **1**, and 1.32% to 65.17% for complex **2**. At low concentrations (from 0.5 to 3.5 μM), the antioxidant activity of complex **1** is higher than complex **2**. These results showed that the suppression ratio increased with increasing sample concentrations in the range of 0.5–4.5 μM. It is believed that the information obtained would be helpful to develop new potential antioxidants and therapeutic agents for some diseases.

4. Conclusion

Two new ruthenium(II) polypyridyl complexes $[Ru(dmp)_2(DNPIP)]^{2+}$ **1** and $[Ru(dmp)_2(DAPIP)]^{2+}$ **2** have been synthesized and characterized. The DNA-binding of these complexes with CT DNA indicated that the two complexes can intercalate between DNA base pairs. Both complexes can bring about cleavage of plasmid DNA when irradiated at 365 nm for 30 min. The studies of mechanism on photocleavage demonstrated that superoxide anion radical ($O_2^{\cdot-}$) and singlet oxygen ($^1O_2$) may play an important role. The data obtained from continuous variation analysis were consistent with a 1:2 and 1:1 [complex]/[DNA] binding mode for complexes **1** and **2**, respectively. Cytotoxicity assay in vitro showed that complex **1** displayed higher antitumor activity than complex **2** against selected tumor cell lines. The cellular uptake indicated that complex **2** can enter into the cytoplasm and accumulate in the nuclei. Antioxidant activity experiments showed that two Ru(II) complexes exhibited good antioxidant activity against hydroxyl radical (·OH).

Acknowledgements

This work was supported by the National Nature Science Foundation of China (Nos. 30800227 and 31070858) and Guangdong Pharmaceutical University.

References

[1] C.S. Allardyce, P.J. Dyson, Platinum Met. Rev. 45 (2001) 62.
[2] J.M. Rademaker-Lakhai, D. Van Den Bongard, D. Pluim, J.H. Beijnen, J.H.M. Schellens, Clin. Cancer Res. 10 (2004) 3717.
[3] G. Sava, A. Bergamo, S. Zorzet, B. Gava, C. Casarsa, M. Cocchietto, A. Furlani, V. Scarcia, B. Serli, B. Iengo, E. Alessio, G. Mestroni, Eur. J. Cancer 38 (2002) 427.
[4] A. Bergamo, R. Gagliardi, V. Scarcia, A. Furlani, E. Alessio, G. Mestroni, G. Sava, J. Pharmacol. Exp. Ther. 289 (1999) 559.
[5] G. Sava, I. Capozzi, K. Clerici, G. Gagliardi, E. Alessio, G. Mestroni, Clin. Exp. Metastasis 16 (1998) 371.
[6] L. Morbidelli, S. Donnini, S. Filippi, L. Messori, F. Piccioli, P. Orioli, G. Sava, M. Ziche Br, J. Cancer 88 (2003) 1484.
[7] I. Bratsos, S. Jedner, T. Gianferrara, E. Alessio, Chimia 61 (2007) 692.
[8] C.G. Hartinger, M.A. Jakupec, S. Zorbas-Seifried, M. Groessl, A. Egger, W. Berger, H. Zorbas, P.J. Dyson, B.K. Keppler, Chem. Biodiversity 5 (2008) 2140.
[9] F.T. Garzon, M.R. Berger, B.K. Keppler, D. Schmaehl, Cancer Chemother. Pharmacol. 19 (1987) 347.
[10] M.R. Berger, F.T. Garzon, B.K. Keppler, D. Schmaehl, Anticancer Res. 9 (1989) 761.
[11] M.H. Seelig, M.R. Berger, B.K. Keppler, J. Cancer Res. Clin. Oncol. 118 (1982) 195.
[12] S. Kapitza, M. Pongratz, M. Jakupec, P. Heffeter, W. Berger, L. Lackinger, B.K. Keppler, B. Marian, J. Cancer Res. Clin. Oncol. 131 (2005) 101.
[13] M.A. Jakupec, M. Galanski, V.B. Arion, C.G. Hartinger, B.K. Keppler, Dalton Trans. (2008) 183.
[14] Y.J. Liu, C.H. Zeng, Z.H. Liang, J.H. Yao, H.L. Huang, Z.Z. Li, F.H. Wu, Eur. J. Med. Chem. 45 (2010) 3087.
[15] C.P. Tan, S.S. Lai, S.H. Wu, S. Hu, L.J. Zhou, Y. Chen, M.X. Wang, Y.P. Zhu, W. Liang, Y.L. Peng, L.N. Ji, A.L. Xu, J. Med. Chem. 53 (2010) 7613.
[16] M.E. Reichmann, S.A. Rice, C.A. Thomas, P. Doty, J. Am. Chem. Soc. 76 (1954) 3047.
[17] H.L. Huang, Z.Z. Li, Z.H. Liang, Y.H. Yao, Y.J. Liu, Eur. J. Med. Chem. (2011) doi: 10.1016/j.ejmech.2011.04.049.
[18] J. Marmur, J. Mol. Biol. 3 (1961) 208.
[19] M. Yamada, Y. Tanaka, Y. Yoshimoto, S. Kuroda, I. Shimao, Bull. Chem. Soc. Jpn. 65 (1992) 1006.
[20] J.B. Bolger, A. Gourdon, E. Ishow, J.P. Launay, Inorg. Chem. 35 (1996) 2937.
[21] J.B. Chaires, N. Dattagupta, D.M. Crothers, Biochemistry 21 (1982) 3933.
[22] A. Wolf, G.H. Shimer Jr, T. Meehan, Biochemistry 26 (1987) 6392.
[23] S. Satyanaryana, J.C. Dabrowial, J.B. Chaires, Biochemistry 31 (1992) 9319.
[24] S. Satyanarayana, J.C. Dabrowiak, J.B. Chaires, Biochemistry 32 (1993) 2573.
[25] G. Cohen, H. Eisenberg, Biopolymers 8 (1969) 45.
[26] M.T. Carter, M. Rodriguez, A. Bard, J. Am. Chem. Soc. 111 (1989) 8901.
[27] P. Job, Ann. Chim. (Paris) 9 (1928) 113.
[28] C.C. Winterbourn, Biochem. J. 182 (1979) 625.
[29] C.C. Cheng, S.E. Rokita, C.J. Burrows, Angew. Chem. Int. Ed. Engl. 32 (1993) 277.
[30] Y.J. Liu, X.Y. Wei, W.J. Mei, L.X. He, Transition Met. Chem. 32 (2007) 762.
[31] Y.J. Liu, C.H. Zeng, J.H. Yao, F.H. Wu, L.X. He, Huang HLChem Biodivers 7 (2010) 1770.
[32] L.F. Tan, X.H. Liu, H. Chao, L.N. Ji, J. Inorg. Biochem. 101 (2007) 56.
[33] Y.J. Liu, X.Y. Wei, F.H. Wu, W.J. Mei, L.X. He, Spectrochim. Acta Part A 70 (2008) 171–176.
[34] C.H. Zeng, Y.J. Liu, Z.Z. Li, Z.H. Liang, H.L. Huang, F.H. Wu, Transition Met. Chem. 35 (2010) 731.
[35] A.E. Friedman, J.C. Chambron, J.P. Sauvage, N.J. Turro, J.K. Barton, J. Am. Chem. Soc. 112 (1990) 4960.
[36] L.S. Lerman, J. Mol. Biol. 3 (1961) 18.
[37] J.K. Barton, A.L. Raphael, J. Am. Chem. Soc. 106 (1984) 2466.
[38] S.A. Lesko, R.J. Lorentzen, P.O. Ts'o, Biochemistry 19 (1980) 3023.
[39] R. Nilsson, P.B. Merkel, D.R. Kearns, Photochem. Photobiol. 16 (1972) 117.
[40] A.K. Patra, M. Nethaji, A.R. Chakravarty, J. Inorg. Biochem. 101 (2007) 233.
[41] X.L. Hong, H. Li, C.H. Peng, J. Mol. Struct. 990 (2010) 197–203.
[42] H.L. Huang, G.P. Tang, Q.Q. Wang, D. Li, F.P. Shen, J. Zhou, H. Yu, Chem. Commun. (2006) 2382.
[43] V. Vijayanathan, T. Thomas, A. Shirahata, T.J. Thomas, Biochemistry 40 (2001) 13633.
[44] T. Sarkar, A.S. Petrov, J.R. Virko, C.T. Santai, S.C. Harvey, I. Mukerji, N.V. Hud, Biochemistry 48 (2009) 667.
[45] C. Santini, M. Pellei, G.G. Lobbia, D. Fedeli, G. Falcioni, J. Inorg. Biochem. 94 (2003) 348.